(Submitted to the Journal of Geophysical Research, July, 1995)

Resonance and Elastic Nonlinear Phenomena in Rock

Paul A. Johnson†, Bernard Zinszner§, and Patrick N. J. Rasolofosaon§

†EES-4, MS D443, Los Alamos National Laboratory, Los Alamos, New Mexico 87545[1]
Tel: (505) 667-8937 Fax: (505) 667-8487
Email: Johnson@seismo5.lanl.gov

§Institut Français du Pétrole, B. P. 311-92506, Rueil Malmaison Cedex, France
Tel: 33 (1) 47-52-68-53 Fax: 33 (1) 47-52-70-60
Email: Bernard.ZINSZNER@ifp.fr, Patrick.RASOLOFOSAON@ifp.fr

---

[1]*also at* Université Pierre et Marie Curie, Department de Recherches Physiques, Tour 22, 4, Place Jussieu, 75252 Paris Cedex 05

Resonance and Elastic Nonlinear Phenomena in Rock

Paul A. Johnson[†], Bernard Zinszner[§], and Patrick N. J. Rasolofosaon[§]

[†]EES-4, MS D443, Los Alamos National Laboratory, Los Alamos, New Mexico 87545
(*also at* Université Pierre et Marie Curie, Bureau des Mécaniques, Tour 22, 4, Place Jussieu, 75252 Paris Cedex 05)
[§]Institut Français du Pétrole, B. P. 311-92506, Rueil Malmaison Cedex, France

Abstract

In the laboratory, rocks display highly elastically nonlinear behavior. Characteristic parameters of nonlinear elasticity can be measured in a resonant bar experiment. Two important features of nonlinear resonant behavior are a shift in resonant frequency away from the linear resonant frequency as the amplitude of the disturbance is increased, and the harmonics in the time signal that accompany this shift. We have conducted Young's mode resonance experiments using bars of a variety of rock types (limestone, sandstone, marble, chalk) and of varying diameters and lengths. Typically, resonant frequency shifts of 10% or more are observed at strains of 10^{-7} - 10^{-6} for samples at a variety of saturation conditions and ambient pressure conditions. Correspondingly rich spectra measured from the time signal progressively develop with increasing drive level. To date, the resonant peak is observed to always shift downward (if indeed the peak shifts), indicating a net softening of the modulus with drive level. This observation is in agreement with our pulse-mode and static test observations, and those of other researchers. Resonant peak shift is not always observed even at large drive levels. This is an unexpected result; however, harmonics are always observed even in the absence of peak shift when detected strain levels exceed 10^{-7} or so. Important implications for measurement of modulus and Q (inverse attenuation) also result from our study. Resonant peak shift may begin at even the lowest drive levels in rock when it occurs, and peak shift and peak width is dependent on frequency sweep direction. Therefore, measurement of moduli and Q must be undertaken with great caution. Ultimately, we hope to apply this technique to characterizing the nonlinear response of rock, to study of progressive change in

material property, to applications in nondestructive evaluation, and to understanding of the nonlinear response of the earth's crust.

Introduction

Observation of nonlinear elastic response in rock is not a new or novel revelation. For example, one well known manifestation of this behavior is demonstrated by countless quasi-static measurements on rock of velocity (or modulus) versus applied stress (e.g., Birch, 1966). These tests show a strong nonlinear dependence between stress and strain (or modulus and stress), in addition to the phenomena of hysteresis and discrete memory [also termed end point memory] (e.g., Holcomb, 1982). These phenomena are due primarily to compliant features in the rock (cracks, grain boundaries, joints, etc.) and fluid effects. More recent dynamic studies of transient waves in rock at atmospheric pressure demonstrate that rock has a large nonlinear response at relatively small strains [e.g., Van Den Abeele, 1994; Guyer et al., 1994; Liu, 1994; Johnson and McCall, 1994; Meegan et al., 1993; Belyaeva et al., 1993; Ostrovsky, 1991; Bakulin and Protosenya, 1991; Bonner and Wanamaker, 1991; Johnson and Shankland, 1989; Zinov'yeva et al., 1989; Beresnev and Nikolaev, 1988; Johnson et al., 1987; Bulau et al., 1984]. The existence of a significant nonlinear elastic response at even moderate strains is not commonly appreciated.

Our intention here is to describe, and in some cases, interpret many manifestations of nonlinear elastic phenomena induced by resonating a bar of rock in Young's mode. We will emphasize resonant peak bending and harmonic generation, but other unexpected, "strange", behavior resulting from resonant excitation as is observed in some rocks such as chalk will also be described. A surprising result of our work is that nonlinear behavior is not necessarily linked with resonant peak bending. That is, resonant peak bending always indicates that the material is responding nonlinearly; however, nonlinear response may exist without measurable resonant peak shift. On the other hand it will also be shown that resonant peak shift may begin at even the

lowest drive levels in rock and that peak shift and peak width is dependent on sweep direction. Therefore, measurement of moduli and Q must be undertaken with great caution.

In section I, the classical theoretical approach to describing a nonlinear oscillator will be illustrated. In section II the experimental procedure will be described. This section will be followed by sections describing the results (section III), discussion (section IV), and conclusions (section V).

I. Theory

Nonlinear resonance has been discussed by many authors and treatments can be found in numerous texts (e.g. Stoker, 1950). It is not our primary purpose here to review theory in detail nor to point out the associated problems one encounters when applying this theory to rock. This has already been done by Guyer et al. (1995) and discussed by Nazarov et al., (1988). Therefore, the nonlinear resonance theoretical development will be only briefly covered in this section.

In the classical approach to describing wave propagation in a nonlinear material, the energy density is expressed as a function of the scalar invarients of the strain tensor (e.g., Landau and Lifshitz, 1959). The strain energy is typically expanded to higher order resulting in an equation of state where stress is expressed as a function of the strain and a series expansion of the modulus. In a typical Young's mode resonance experiment, the bar is secured in the middle, excited at one end and the acceleration is detected on the opposite end. Following Landau and Lifshitz (1959) and Guyer et al. (1994), the energy density E is,

$$E = -\mu\varepsilon^2_{ik} + \left(\frac{K}{2} - \frac{\mu}{3}\right)\varepsilon^2_{il} + \frac{A}{3}\varepsilon_{ik}\varepsilon_{il}\varepsilon_{kl} + B\varepsilon^2_{ik}\varepsilon_{il} + \frac{C}{3}\varepsilon^2_{il} + ... \quad (1)$$

the stress tensor σ is,

$$\sigma_{ik} = \frac{\partial E}{\partial(\partial u_i/\partial x_k)} \tag{2}$$

and the equation of motion for the displacement field u is,

$$\rho_o \frac{\partial^2 u_i}{\partial t^2} = \frac{\partial \sigma_{ik}}{\partial x_k} \ . \tag{3}$$

K and μ are the Bulk and shear moduli, respectively; A, B, and C are the third order nonlinear coefficients used by Landau and Lifshitz; ρ_o is the mass density; and ε is the Lagrangian strain tensor,

$$\varepsilon_{ik} = \frac{1}{2}\left(\frac{\partial u_i}{\partial x_k} + \frac{\partial u_k}{\partial x_i} + \frac{\partial u_l}{\partial x_i}\frac{\partial u_l}{\partial x_k} \right). \tag{4}$$

[Einstein summation is assumed]. Using the above expansion gives the one dimensional equation of motion for the displacement field of

$$\frac{\partial^2 u_i}{\partial t^2} = \frac{\partial}{\partial x}\left(c^2 \frac{\partial u}{\partial x} \right), \tag{5}$$

where

$$c^2 = c_o^2 \left[1 + \beta \left(\frac{\partial u}{\partial x} \right) + \delta \left(\frac{\partial u}{\partial x} \right)^2 + \ldots \right], \tag{6}$$

and c is the perturbed wave speed, c_o is the unperturbed wave speed, and β and δ are coefficients that characterize the cubic and quartic anharmonicities (they are the nonlinear coefficients that can be directly related to A, B, and C above [e.g., see Green, 1973; Johnson and Rasolofosaon, 1994). In the classical treatment, the average of the strain field over one period is assumed zero (it may not be), so the quadratic term β is eliminated[2]. Therefore, using classical theory it is the determination of δ that is the goal of the resonance experiment. Following Guyer et al., the term proportional to δ can be replaced by its time average value,

$$\delta \left| \left(\frac{\partial u}{\partial x}\right)^2 \right| \sim \delta \varepsilon^2, \tag{7}$$

and Eq. (6) can be rewritten as,

$$\frac{c^2 - c_o^2}{c_o^2} \sim \frac{\omega^2 - \omega_o^2}{\omega_o^2} \sim 2\left[\frac{\omega - \omega_o}{\omega_o}\right] \sim 2\left[\frac{\Delta\omega}{\omega_o}\right] \sim \delta\varepsilon^2, \tag{8}$$

where ω_o is the angular frequency of the "linear" resonant peak and ω is the angular frequency of the resonant peak as it shifts with driving amplitude. Our experiments are configured to measure Q, ω and ω_o and the acceleration $\left(\partial^2 u/\partial t^2\right)$ at any desired drive level or frequency. Therefore, we can, in theory, determine δ, the cubic nonlinear modulus. We are also capable of measuring the harmonic amplitudes of the time signal when the resonance is at maximum value. Therefore, as a comparison we can obtain an approximation of δ from measurement of the third harmonic amplitude,

$$\delta \sim -\frac{\left(\partial^2 u_3/\partial t^2\right)\omega_o^4 L^2}{\left(\partial^2 u_1/\partial t^2\right)^3}, \tag{9}$$

---

[2]It can be shown that including the quadratic term results in the same dependence in ε.

where L is the bar length, $\left(\partial^2 u_3/\partial t^2\right)$ is the acceleration of the third harmonic at resonance, and $\left(\partial^2 u_1/\partial t^2\right)$ is the acceleration of the fundamental frequency at resonance. Similarly, from the second harmonic amplitude we can obtain an approximation of β:

$$\beta \sim -\frac{\left(\partial^2 u_2/\partial t^2\right)\omega_o^2 L}{\left(\partial^2 u_1/\partial t^2\right)^2}. \qquad (10)$$

Eq. (5) is hysteretic in its frequency behavior (not to be confused with hysteresis in stress versus strain!) in that it depends on which direction the driving frequency is swept, meaning that the amplitude is not uniquely determined by the applied forcing function. This is a classical result from analysis of nonlinear oscillators (e.g., Stoker, 1955). This behavior will be illustrated in the results section.

The discrete system assumption implies that stress σ, strain ε, and displacement u are homogeneous in the sample as a function of time. In reality, this is not the case. Stress and strain are maximum at the center of the bar (in absolute value) and minimum at the bar ends. Displacement is maximum at the bar ends and minimum in the bar center; however, solution to the elastic resonance equation of motion provides nearly identical results to those above.

Young's modulus E_o is obtained from the fundamental resonant frequency measured at low drive voltage in the strain interval of 10^{-8}-10^{-9} (linear regime). From the mass density ρ and length L the modulus is,

$$E_o = \rho_o C_E^2 = \rho_o \frac{L^2 \omega_o^2}{\pi^2} \qquad (11)$$

where ω_o is the fundamental resonant bar frequency at linear elastic strain, and C_E is the Young's mode velocity at ω_o.

II. Experimental Procedure

The basic elements of the experimental configuration for obtaining frequency versus acceleration measurements are shown in Figure 1. We use both an analog or digital experimental apparatus, depending on the desired result. In general, the analog method is superior when it is necessary to observe a large dynamic range. The digital method is fast and convenient, but has the disadvantage of a smaller dynamic range.

The analog method is described first. Two function generators serve as a voltage to frequency converter. A ramp voltage function output from one function generator is fed to a second function generator to create a frequency sweep interval. The interval is chosen to encompass frequencies well above and well below the fundamental resonant mode of the sample. The signal is amplified and acoustically excited by an electromagnetic (coil/ magnet) source and affixed oriented parallel to the axis of the sample. Piezoelectric and shaker-type sources are also used. The signal is detected by use of a calibrated accelerometer, is pre-amplified, and is then fed to a voltmeter where the signal is time averaged and frequency versus maximum acceleration is plotted on a graphics tablet. The signal is also fed to a digital oscilloscope for monitoring the time series signal. Measurements are made of both upward and downward frequency sweeps over the chosen interval. Typically, 5-20 experiments are conducted at successively increasing drive voltages over the same frequency interval in order to monitor resonant peak shift and harmonic generation. A single sweep is typically 1-5 minutes in duration.

The digital measurements are made with a PC that contains a card that has both a function generator and a heterodyne detector. In this configuration, a constant amplitude drive signal output from the card is multiplied with the detected signal from the rock. The multiplied signal is time averaged and low-pass filtered providing a dc output proportional to the detected

acceleration. The PC also contains a 16 bit A-D card for capturing time signals for harmonic analysis. A stand alone spectral analyzer that has stacking capability is also used when desired.

Measurements of at least nine different rock samples were made. These include Berea sandstone, Meule sandstone, Lavoux limestone, magnesium marble, Estaillades limestone, St. Pantaleon limestone, Asian marble, Chalk, Fontainebleau sandstone and Carrera marble. Comparative studies were conducted using the relatively elastically linear materials aluminum, PVC, Plexiglas, Pyrex glass, porous sintered aluminum, and polycarbonate. For several rock samples, including Meule sandstone, Lavoux limestone, and chalk, measurements were taken at numerous different water saturation levels between approximately 1-99%. In each case, the sample was saturated after evacuation and measurements were made as the rock dried under room conditions. Densities were estimated from the dry weight and the measured porosity. Sample lengths ranged from 0.30 - 1.15 m and diameters ranged from 0.025 - 0.105 m.

III. Results

Typical Behavior of Elastically "Linear" Solids

Figure 2a shows a sample sequence of resonance curves for twelve different excitation levels in polyvinyl chloride (PVC), a material that is relatively "linear" in comparison with most rocks. The figure shows detected acceleration versus swept frequency. Both downward and upward frequency sweeps were conducted at each drive level. Downward and upward sweeps are indistinguishable from each other. Note the Q (59) is similar to many rocks. Figure 2b shows excitation-strain data collected at the resonant peak excitations in polycarbonate, another "linear" material, from a nearly identical experiment to that shown in Figure 2a [the resonant peaks are of the same character as those for PVC, i.e., no peak bending is observed]. Note that the excitation versus strain curve is in essence a net stress versus strain curve because excitation is linearly proportional to stress. The experiment differs slightly in that, at each resonant peak, the

drive frequency and excitation level is held constant while the time signal is collected and averaged to improve the signal to noise ratio. The averaged signal is then Fourier analyzed and the relative harmonic amplitudes are measured. The plot shows the drive excitation level in mA on the left-hand Y-axis versus the measured strain level on the X-axis (solid bold line). In this strain range, no harmonics are observed. It comes as no surprise that all of the "linear" materials studied have a constant derivative of $\partial(\text{excitation})/\partial\sigma$, that is, a linear stress-strain relation and therefore a single modulus (See below). This plot will be compared to that for a rock shortly.

Strain ε is calculated as follows,

$$\varepsilon = \frac{\partial u}{\partial x} = \frac{2u}{L_o}, \tag{12}$$

where again u is displacement and L_o is the bar length at rest. The factor of 2 appears because the strain is symmetric about the center of the bar. Acceleration

$$\frac{\partial^2 u}{\partial t^2} = -u\,\omega^2\, e^{i\omega t} \tag{13}$$

is the actual measured value in the experiments, however, for a continuous wave drive. For the time averaged signal, the displacement at the bar ends is,

$$u = -\frac{\partial^2 u/\partial t^2}{\omega^2} \tag{14}$$

where ω is the frequency at which the acceleration is measured (the maximum resonance response in general). From Eqs. (12) and (14) strain is then,

$$\varepsilon = \frac{\partial u}{\partial x} = \frac{2u}{L_o} = -2\,\frac{\partial^2 u/\partial t^2}{L_o\omega^2}\ . \tag{15}$$

We indicate several important observations from Figures 2a and 2b that can be regarded as representative for "linear" solids. In general, these materials:

(1) show no detectable peak bending;

(2) display a linear relationship between excitation and strain;

(3) show a very low level of harmonics compared to nonlinear elastic materials.

Based of the resolution of our system we consider that the level of harmonic generation in "linear" solids is near the limit of our resolution (using a 12 bit digital oscilloscope and averaging signals).

These four observations are representative of all of the "linear" materials listed above[3]. When harmonics are observed in these materials, they are inferred to originate from the response of the materials themselves because harmonics are not observed in all of the "linear" materials (e.g., sintered aluminum), and the relative harmonic levels vary from material to material. This would not be the case if the source (especially electro-magnetic hysteresis) or electronics were the source or the harmonics. Based on our research, that of Nazarov et al. (1988), and that from the nonlinear acoustics community, we would not expect to observe harmonics in these materials. We believe there may be geometrical "extrinsic" effects in resonance that induce small levels of harmonics as opposed to material property "intrinsic" effects that do not contribute to harmonic generation in these materials. This work is continuing. The results of attenuation, sample dimensions, frequency shift, modulus, detection of harmonics, and strain levels on elastically "linear" materials are displayed in Table 1.

Typical Behavior of Elastically Nonlinear Solids: Rock

In Figure 3a, a representative result for Young's mode resonant behavior in rock is shown. The material is Lavoux limestone under ambient conditions. Contrast this result to that

[3]A cautionary note: the experimental apparatus does not provide the frequency resolution to quantitatively study high Q materials such as Aluminum.

of PVC shown in Figure 2a. The difference is astonishing. Figure 3b shows the result for Fontainebleau sandstone also at ambient conditions. The central portion of Figure 3b shows the resonant peak bending, and the bottom and top plots show the corresponding time and frequency domain signals at low (but nonlinear) drive level, and large drive level, respectively. Note that the linear resonant response has been expanded vertically in both Figure 3a and 3b.

Peak Bending and Frequency Hysteresis in Rock

In the resonance plots shown in Figures 3a and 3b, the solid lines represent downward frequency sweeps and the dashed lines represent upward frequency sweeps. Two striking observations are of note. First, the peak bending is dramatic as a function of detected acceleration in these samples. Second, the shape of the curve depends on in which direction the sweep takes place, upward or downward in frequency. This second observation is typical of nonlinear oscillators in general (e.g., see Stokes, 1950). Qualitatively, the resonant frequency shift and the difference in upward and downward resonant behavior (frequency hysteresis) can be thought of as follows. Initially, the modulus is in its at rest (elastically "linear") state. At very low, but successively increasing drive levels, the resonant response *may* (but not always) remain at the same frequency, as has been shown by others (e.g., Winkler and Nur, 1979; Murphy, 1982; Bulau et al., 1984). As the source drive level is increased, the material net modulus begins to drop, and this is reflected in a drop in the resonant frequency. As the drive frequency approaches the modified resonant frequency, naturally, the excitation becomes larger as well. Larger excitation induces the net modulus to drop even further, and the resonant frequency in effect, "chases" the resonant peak as it steadily shifts downward in response to larger and larger excitation. This cause and effect relationship takes place until the bar reaches some maximum energy state proportional to the maximum input energy in the sample. At this point, as the frequency is decreased further, it passes through the modified resonant peak and the amplitude drops rapidly back to the non-resonant value. The resonance frequency immediately shifts back to its original, elastically "linear" value. The shift back can be readily observed by conducting a low

amplitude frequency sweep immediately after a high amplitude sweep. The resonant frequency is that of the original value, or very close to it.

As frequency is swept in the upward direction, the modulus begins again at its rest (elastically linear) state. At larger excitation levels, as the frequency approaches the linear resonant value and more energy is introduced into the resonating bar, the net modulus begins to drop as before. In effect, the maximum energy state (depending on drive level and material property) where the resonant frequency is at minimum (as is the modulus) and the upward swept frequency "meet" and the frequency passes through the modified resonant peak. This process takes place over a very short frequency interval as can be seen by the abrupt increase in acceleration response in Figure 3a. As frequency increases further, the resonant peak is modified upward, but lags behind the sweep frequency in the experiments shown. As before, the modulus returns to its at rest state after excitation.

The corresponding time and frequency domain plots (Figure 3b bottom and top plots) for two different resonance peaks corresponding to two different excitation levels show typical results. In this case, at low drive (but in the nonlinear response regime), the time signal is distorted, being composed of the fundamental and third harmonic. As the drive is increased, the time signal becomes highly distorted, is asymmetric and has a dc component, all manifestations of elastic nonlinear behavior in the material. The corresponding spectrum illustrates the rich spectrum associated with large excitation level. In general, odd harmonics tend to dominate in rock, in contrast to the elastically "linear" materials studied above.

Figure 4 shows the excitation and harmonic ratio versus strain for the Lavoux Limestone sample at 0.5% water saturation. In this case, only the second and third harmonics were measured although higher harmonics were present. The excitation versus strain curve is not atypical of rocks. Often, for the rocks studied and at the various saturation conditions, the excitation goes approximately as the square of the strain. There are certainly exceptions to this, one being chalk (to be discussed soon). Also, note that the third harmonic grows much more rapidly than the second harmonic as was noted previously.

We indicate three fundamental observations from Figures 3a and 4 that can be regarded as representative for rock. These materials:

(1) generally but not always show peak bending;

(2) generally but not always display a nonlinear relationship between excitation and strain over the strain intervals studied, indicative of a nonlinear relation between stress and strain (see below); and,

(3) show a rich spectrum of harmonics at strain levels as low as 10^{-7}.

A final observation in regards to resonant peak shift is noteworthy. Depending on the rock and the saturation state, the resonant peak may begin shifting immediately, even at the lowest possible applied drive levels and at strain levels that are extremely small ($<10^{-8}$). This is certainly not an exceptional observation in the rocks that were studied. For example, Berea sandstone shows this behavior at ambient conditions. This is an important consideration for measurement of Q and velocity when applying the resonant bar method.

The Change in Resonant Frequency, Harmonics, and the Nonlinear Modulus

As indicated from the approximation shown in Eq. (8), the cubic nonlinear parameter δ should be obtained from the change in angular resonant frequency ω as a function of the strain ε. Comparison can be made with δ obtained from measurement of the third harmonic amplitude (Eq. (9)). The quadratic nonlinear parameter β should be obtained from the second harmonic amplitude (Eq. (10)). Higher order nonlinear parameters may exist based on the observation of higher harmonics. The theory describing the higher order moduli using a perturbative expansion approach is derived in Van Den Abeele (1995). An alternative is a discontinuous equation of state which requires only a quadratic term in strain (see Guyer et al., 1995).

We plot $\Delta\omega/\omega_o$ versus strain ε for several data sets. Meule sandstone, Lavoux limestone, St. Pantaleon limestone, Fontainebleau sandstone, and chalk are shown at various saturation conditions in Figure 5 Two observations are of note.

(1) $\Delta\omega/\omega_o$ does not go as the strain squared but is an approximately linear function of the strain with of slope of approximately 0.7-1.5.

(2) At large strain, the slope of $\Delta\omega/\omega_o$ versus strain ε tends to decrease.

The error bars are very small at large $\Delta\omega/\omega_o$ (approximately the diameter of the symbols), but are large at small $\Delta\omega/\omega_o$ (up to a factor of two). Despite this, it is convincing from the large number of data that the slope is not two. This implies the traditional theory is inadequate for obtaining the nonlinear modulus form the resonant peak shift in its current state of development.

Figure 6 shows how the cubic nonlinear parameter is estimated for Berea sandstone, based on Eq. (9). A similar plot can be made using the second harmonic data using Eq. (8) to obtain the quadratic parameter. The outstanding result from Figure 6 is that the cubic parameter is impossibly large ($> |10^{10}|$). The results for various rocks are tabulated in Table 2 along with their saturation states, Q, and the nonlinear modulus obtained from harmonic analysis using Eqs. (9) and (10) for data where harmonics were available. Table 3 shows the results for Lavoux limestone at all saturation states. The nonlinear coefficients derived from the slope change and the harmonics are far too large to be compatible with other data. We will address this issue in the discussion.

Ultrasonic Pulse-Mode Velocity Change With Excitation Level

It is an interesting exercise to measure the velocity as a function of the excitation and strain level in rock, because we expect such a change. In this experiment, we placed piezoelectric transducers on either side of the bar near the bar midpoint for lateral measurement of time delay. We then conducted the resonant sweep measurements at steadily increasing drive levels as before. The pulse-mode wave time delay across the sample is measured when the bar is at peak resonance for each respective excitation level. The experiment is duplicated with transducers very near one end of the bar. The two data sets were collected intentionally where the stress is maximum (bar center) and minimum (bar end). We would expect to see a larger effect where the stress is largest, if at all.

The results are shown in Figure 7a. Errors in measurements are much smaller than the overall change. As expected, there was no measurable change in velocity recorded near the bar end. At the bar center, the modulus decreases as a function of excitation level (the normalized lateral modulus is related to the longitudinal modulus by Poisson's ratio, a nonlinear quantity also). This is consistent with all results we are aware on rock in that it demonstrates a softening nonlinearity of the rock.

The β based on the change in velocity (modulus) is approximately 10^4, a value compatible with static and quasi static results.

Strange Nonlinear Elastic Behavior: Chalk

In our investigation we have discovered some additional unexpected results that seem to be related to rock composition. Chalk is an example of a rock that shows unique "strange" behavior relative to the other rocks investigated. An illustration of a sample resonance curve for chalk at a water saturation of about 45% is shown in Figure 8a. Only the "linear" resonance peak (expanded vertical scale) and one high drive level sweep, both upward and downward, are shown. The frequency changes from approximately 1260 to 1225 Hz. There are three striking observations that can be made from this plot and from our general experience with chalk.

(1) The curves do not resemble those of other rocks; in fact, the curves are an approximate mirror image of the typical behavior in rock. The abrupt transition in amplitude occurs on the high frequency side of the nonlinear resonance (compare the plot for Fontainebleau sandstone in Figure 3a).

(2) The ratio of the low amplitude "linear" strain level to the large amplitude strain level is significantly larger when compared to other rocks (not shown).

(3) At large drive level during the downward sweep, the detected signal response oscillates rapidly up and down as it approaches the resonance peak.

The harmonic spectrum which was observed but not collected for a different but similar experiment is enormously rich. Harmonics are observed out to at least 50 kHz. Figure 8b shows

the excitation level versus strain versus harmonic rations. Note again the nonlinear excitation-strain curve. Figure 8c shows a plot of the harmonic spectrum for an experiment with dry chalk. The plot shows $\Delta\omega/\omega_o$ versus strain versus harmonic ratio for a sample at 0.5% water saturation. The result shown is typical for a dry sample. Interestingly, in contrast to the partially saturated chalk, there is very little resonant peak bending; however, the harmonic spectrum is nonetheless extremely rich. Figure 8d shows a comparative plot for Lavoux limestone (0.1% saturation). Peak bending and harmonic generation both occur in the Lavoux which is typical of a rock; whereas, peak bending is nearly negligible in the chalk while the harmonic spectrum is rich.

The oscillation in the response for partially saturated chalk shows an instability not obviously present in other rocks. We can only infer that chalk has perhaps the most nonlinear response of any rock we have investigated as demonstrated by the harmonic content. The instability may be indicative of the onset of chaotic behavior. We were unable to collect spectra in this region of the curve so this hypothesis is currently not verified.

It is not obvious why the resonant response of chalk is the reverse of that for other rocks. Future modeling may help us understand this phenomenon. We can infer from the results for chalk that much of the energy input into chalk at the fundamental or near the fundamental resonance is transferred to harmonics, far more so than in other materials studied. This is especially true of partially saturated chalk where the large drive level resonant peak shows a lower response in acceleration than the low amplitude drive. The associated spectrum confirms this. An important lesson from the chalk is that nonlinearity is not necessarily indicated by peak bending, but by monitoring harmonics and that saturation plays an important role in the response of the material. This is a very important clue to our later discussion on why the perturbation theory alone is not suitable for rocks.

IV. Discussion

The nonlinear coefficients derived from a perturbation expansion of the resonance wave equation are not realistic in comparison to those obtained from quasi-static experiments. They cannot be correct if we believe the available data from stress-strain tests. We calculate a quadratic nonlinear parameter β of order -10^3 to -10^4 and cubic parameters δ of -10^6 to -10^8 from a diverse suite of data available in the literature for many rock types. Comparison of the stress-strain curve for "normal" nonlinear parameters versus those obtained from resonance are shown in Figure 9. This behavior is not realistic. Other clues indicating that a model invoking a classical perturbation expansion of the equation of state (or the strain energy function) is not correct come from some of the results presented in this work. For example, the observation in chalk of a rich harmonic spectrum in the presence of little or no peak bending is one indication. The incorrect power law dependence as predicted by Eq (8) and shown by the plots in Figure 5 provides an additional and closely related clue. Evidence from elsewhere suggesting that a straightforward perturbation expansion is insufficient comes from the large body of published results showing that hysteresis and discrete memory are ever-present in rock (see e.g., Guyer et al., 1995; Boitnott, 1993; Holcomb, 1982).

What are the implications of the existence of hysteresis and discrete memory in a resonating or propagating wave? These are mechanisms for additional wave distortion (harmonics). Inclusion of discrete memory and hysteresis offers tool whereby a more comprehensive description of nonlinear behavior emerges. The discussion of the theory has been covered elsewhere (Guyer et a., 1995) and it is not our intention to provide the details of the model here. Suffice it to say that the model shows development of harmonics by expanding the modulus to first order with the inclusion of hysteresis and discrete memory. The theoretical results show a rich spectrum of higher harmonics. In fact, Guyer and McCall (1994) have included hysteresis and discrete memory in the nonlinear wave equation for propagating waves. Hysteresis and discrete memory provide a model where harmonics are generated from the nonlinear stress-strain curve and from the cusps of the hysteresis loop (discrete memory). However, the inclusion of hysteresis and discrete memory in the perturbation expansion is not

sufficient as yet in providing us with the tools to directly calculate the nonlinear coefficients in our work. Our theoretical approach is under appropriate modification at present.

Our work shows further that, because the classical theory may not be directly applied to rock, the information about the nonlinear response of a given rock sample is not necessarily obtained in a straightforward manner as it would be in a material that does not display hysteretic and discrete memory effects. Thus application of this method at present is perhaps best suited to comparative study of rocks.

Modulus and Excitation Versus Strain

The excitation-strain curve, for example that shown in Figure 4 for Lavoux limestone, provides some measure of the instantaneous modulus. This makes intuitive sense because, as the excitation increases, energy is transferred into harmonics. The result of measuring the fundamental amplitude is that the calculated strain is smaller than predicted in the absence of energy transfer to harmonics, i.e., in the absence of elastic nonlinearity. The strain at the fundamental frequency is smaller than it should be for a given excitation. Thus the deviation from linearity in the excitation-strain curve is a measure of the energy transfer, in other words, the nonlinearity itself. We can be certain that the curve is not a source or instrumentation effect based on the elastically "linear" materials we have studied. Figure 2b shows such an example for sintered aluminum. The excitation-strain curves could be used to calculate nonlinear moduli β and δ because excitation can be directly related to applied force; however, if hysteresis and discrete memory are active, then this would not be a useful exercise because the downgoing curve for excitation-strain would differ, and we are unable to measure the strain in this direction.

Lessons For Measurement of Q and Modulus

An important lesson from observation of peak bending is that Q cannot be reliably measured in this circumstance. The imaginary portion of the nonlinear modulus is the attenuation, and it is related in a very complex manner to the width of the peak and the associated

harmonics (e.g., McCall, 1994; Van Den Abeele, 1995). Therefore, measurement of Q for anything but a perfectly linear (i.e., symmetric) resonant curve is meaningless. In fact, even applying the results of an apparent linear resonance curve can be misleading. As our experience with chalk shows, it is possible to observe little or no resonant peak bending simultaneous with even enormous harmonic generation. The presence of harmonics will result in an underestimate of Q.

Sweep Rate and Relaxation Effects

We have not addressed sweep rate effects in this paper. We have examined rate dependence, and have observed obvious rate-dependent effects on the resonance curves. The resonance curves maintain the same general character if, for example, the sweep rate is increased. Our experiments were conducted at rates we deemed reasonable after numerous empirical tests. In addition, we have observed relaxation effects after a frequency sweep in some rocks. We have noted that it may take tens of seconds or up to several minutes for a rock to return to its original "linear" elastic state after a large amplitude frequency sweep. In any case, these effects do not affect the conclusions presented here.

Relative Strain Levels

What is the relation between large strain quasi-static tests and wave measurements that are conducted at orders of magnitude smaller strain levels? We believe the link between large and small strain level measurements has been made with the introduction of the hysteresis and discrete memory model proposed by McCall and Guyer (1994) and Guyer et al. (1995). In this work, a framework for understanding nonlinear elasticity is presented, including an understanding of the continuum between large and small strain measurements, and the relation between the elastic makeup of the material, hysteresis, and discrete memory.

Of What Use are Nonlinear Elastic Measurements?

A fundamental question remains as to the value of measuring and understanding nonlinear elasticity in rock over and above academic interest. To first order, the nonlinear elastic response is certainly related to the micro and macro structure of the material, the grain to grain contacts, the microcracks, joints, etc. The contained fluid also plays a very important role. The sensitivity of the nonlinear response to the structure and fluid content is far larger than that of standard linear measurements of wave speed, modulus and attenuation. The problem is that these measurements are difficult to make and great care must be taken in separating the apparatus effects that can be identical. These are problems that are surmountable. The rewards may be great. We believe that the work presented in this paper and work on nonlinear elasticity by our group and other groups will lead us to a new level of understanding the makeup of materials; new methods of quantifying the features that contribute to the nonlinear response in manners that were previously unrealized by application of linear methods. The discipline of nonlinear elasticity is coming ever closer to this goal.

V. Conclusions

We have demonstrated that the classical approach to modeling nonlinear oscillators does not hold for rocks. We believe the key difference between rocks and a classic nonlinear oscillator is the presence of discrete memory and hysteresis in rock. We have also shown that great care must be taken when measuring and interpreting modulus and Q from resonance experiments. This is not a new result (e.g., Winkler and Nur, 1979, etc.); however, it is clear from our work that initiation of peak bending cannot be relied on for the onset of nonlinear elastic response. On the contrary, the only reliable method is to monitor harmonic generation.

The ramifications of nonlinear response in rock may ultimately effect many areas of research in Geoscience including seismology, where the spectral distortion of seismic waves during propagation must be considered (e.g., Johnson and McCall, 1994; Balau et al., 1984). This was recently field verified by Beresnev and Wen. Other areas of research include rock

mechanics and materials science where the nonlinear response of a material may be used for characterization purposes. In addition, characterization of material property change by monitoring nonlinear response may be of value. For instance, these changes include variations in water saturation for porous media, change in response to variations in stress, change induced by fatigue damage, etc. Work in these areas is ongoing.

Acknowledgments. This work was performed under the auspices of the Offices of Basic Energy Research, Engineering and Geoscience (contract W-7405-ENG-36), US. Department of Energy with the University of California, and the Institut Français du Pétrole. We thank Michel Masson for experimental assistance, and Thomas Shankland, Albert Migliori, Koen Van Den Abeele, and James Ten Cate for helpful discussions. We thank G. D. Meegan who originally suggested conducting the experiments. We are deeply indebted to Katherine McCall and Robert Guyer who have contributed much to our understanding of the phenomena described here.

References

Bakulin V. N. and A. G.. Protosenya, Nonlinear effects in travel of elastic waves through rocks, *Transactions (Doklady) of the USSR Academy of Sciences, Earth Sciences Sections , 263*, 314-316 (1981).

Beresnev, I. A. and A. V.. Nikolaev, Experimental investigations of nonlinear seismic effects, *Phys. of the Earth and Planetary Int., 50*, 83-87 (1988).

Beresnev, I. A., and K-L. Wen, The possibility of Observing nonlinear path effects in earthquake-induced seismic wave propagation, Bull. Seism. Soc. Am., *in review* (1995).

Birch, F., in *Handbook of Physical Constants* , Ed. Clark, S. P. , Jr., Geol. Soc. Am. Press, Connecticut, 97-174 (1966).

Boitnott, G. N., Fundamental observations concerning hysteresis in the deformation of intact and jointed rock with applications to nonlinear attenuation in the near source region, *in Proceedings of the Numerical Modeling for Underground Nuclear Test Monitoring Symposium, Durango, CO., 1993, S. R. Taylor and J. R. Kamm, Eds., Los Alamos National Laboratory Report LA-UR-93-3839* (1993).

Bonner B. P. and B. J.. Wanamaker, Acoustic nonlinearities produced by a single macroscopic fracture in granite, in *Review of progress in quantitative NDE,* edited by D. O.. Thompson and D. E.. Chimenti, Plenum, New York, *10B*, 1861-1867 (1991).

Bulanov, V. A., Acoustical nonlinearity of microinhomogeneous liquids, in *Advances in Nonlinear Acoustics* , H. Hobaek, Ed., World Scientific, Singapore, 674-678, 1993.

Bulau, J. R., B. R. Tittmann, and M. Abdel-Gawad, Nonlinear wave propagation in rock, *Proceedings of the 1984 IEEE Ultrasonics Symposium*, 775-780 (1984).

Day, S. M. and J. B. Minster, Numerical simulation of attenuated wavefields using a Pade approximation method, *Geophys. J. R. Astr. Soc. 78*, 105 (1984)

G.P. Zinov'yeva, I.I. Nesterov, Y.L. Zdhakhin, E.E. Artma, and Y.V. Gorbunov, *Transactions (Doklady) of the USSR Academy of Sciences, Earth Science Sections* **307** (1989) 337.

Gol'dberg, Z. A., Interaction of plane longitudinal and transverse elastic waves, *Sov. Phys. - Acoustics, 6*, 307-310, 1959.

Green, R. E. Jr., *Treatise on materials science and technology, Vol. 3, Ultrasonic investigation of mechanical properties* , Academic Press, New York (1973).

Guyer, R. A., K. R. McCall, and G. N. Boitnott, Hysteresis, discrete memory and nonlinear wave propagation in rock, *Phys. Rev. Let.*, in review, 1994).

Guyer, R. A., K. R. McCall, P. A. Johnson, P. N. J. Rasolofosaon, and B. Zinszner, Equation of state hysteresis and resonant bar measurements on rock, *1995 International Symposium on Rock Mechanics, in review*, 1994.

Guyer, R. A., K. R. McCall, P. A. Johnson, P. N. J. Rasolofosaon, and B. Zinszner, Equation of state hysteresis and resonant bar measurements on rock, *1995 International Symposium on Rock Mechanics, in press*, 1995.

Hamilton, M. F., Fundamentals and applications of nonlinear acoustics, in *Nonlinear wave propagation in mechanics -- AMD- 77* , The American Society of Mechanical Engineers, New York, 1986.

Holcomb, D. J., Memory, relaxation, and microfracturing in dilatant rock, *J. Geophys. Res.*, 86, 6235 (1981).

Johnson, P. A. and K. R. McCall, Observation and implications of nonlinear elastic wave response in rock, *Geophys. Res. Let. 21*, 165-168 (1994).

Johnson, P. A. and K. R. McCall, Observation and implications of nonlinear elastic wave response in rock, *Geophys. Res. Let. 21*, 165-168, 1994.

Johnson, P. A. and P. N. J. Rasolofosaon, Nonlinear elasticity and stress-induced anisotropy in rock, *J. Geophys. Res.* in review (1995).

Johnson, P. A. and T. J.. Shankland, Nonlinear generation of elastic waves in granite and sandstone: Continuous wave and travel time observations, *J. Geophys. Res. 94*, 17,729-17,733 (1989).

Johnson, P. A., P. N. J. Rasolofosaon, and B. Zinszner, Measurement of nonlinear elastic response in rock by the resonant bar method, in *Advances in Nonlinear Acoustics* , H. Hobaek, Ed., World Scientific, Singapore, 531-536 (1993).

Johnson, P. A., P. N. J. Rasolofosaon, and B. Zinszner, Measurement of nonlinear elastic response in rock by the resonant bar method, in *Advances in Nonlinear Acoustics* , H. Hobaek, Ed., World Scientific, Singapore, 531-536, 1993).

Johnson, P. A., T. J.. Shankland, R .J.. O'Connell, and J. N.. Albright, Nonlinear generation of elastic waves in crystalline rock, *J. Geophys. Res., 92*, 3597-3602 (1987).

Landau, L. D. and E. M. Lifshitz, *Theory of elasticity, 3rd edition* , Pergamon Press, Oxford (1986).

Liu, F., Nonlinear Elasticity, seismic anisotropy and petrophysical properties of reservoir rocks, Ph.D. Dissertation, Stanford University, 1994.

McCall, K. R. and R. A. Guyer, Equation of state and wave propagation in hysteretic nonlinear elastic material, *J. Geophys. Res.*, in press (1994).

McCall, K. R., Theoretical study of nonlinear acoustic wave propagation, *J. Geophys. Res. 99*, 2591-2600, 1993.

Meegan, G. D., P. A. Johnson, R. G. Guyer, and K. R. McCall, Observations of nonlinear elastic wave behavior in sandstone, *J. Acoust. Soc. Am*. *94*, 3387-3391 (1993).

Murnaghan, F. D., *Finite Deformation of an elastic solid*, Wiley, New York (1951).

Murphy, W. F. III, Ph.D. Dissertation, Stanford University (1982).

Nazarov, V.E., L. A. Ostrovsky, I. A. Soustova, and A. M. Sutin, Nonlinear acoustics of micro-inhomogeneous media, Phys. Earth Planet. Int. 50, 65-73 (1988).

Ostrovsky, L. A., Wave processes in media with strong acoustic nonlinearity, *J. Acoust. Soc. Am., 90*, 3332-3337 (1991).

Polyakova, A. L., Nonlinear effects in a solid, *Sov. Phys. - Solid State 6*, 50-54 (1964).

Stoker, J. J., *Nonlinear Vibrations in Mechanical and Electrical Systems* , 81 pp., Interscience Publishers, Inc., New York (1950).

Toksoz, M. N. and D. H. Johnston, Eds., *Seismic wave attenuation*, Geophysics Reprint Series 2, Soc. Exploration. Geophys. (1981).

Van den Abeele, K. E-A., Elastic pulsed wave propagation in media with second or higher order nonlinearity. part 1: theoretical framework, J. Acoust. Soc. Am., *in review* (1995).

Winkler, K., A. Nur, and M. Gladwin, Friction and seismic attenuation in rocks, *Nature 277*, 528-531, 1979.

Zinov'yeva, G. P., I. I.. Nesterov, Y. L.. Zdhakhin, E. E.. Artma, and Y. V.. Gorbunov, Investigation of rock deformation properties in terms of the nonlinear acoustic parameter, *Transactions (Doklady) of the USSR Academy of Sciences, Earth Science Sections 307*, 337-341 (1989).

Figure Captions

Figure 1. Experimental configuration. See text for explanation.

Figure 2a. Detected acceleration versus swept frequency for a sequence of resonance curves at twelve different excitation levels in polyvinyl chloride (PVC). Both downward and upward frequency sweeps are plotted; however they are indistinguishable from each other. (2b) Excitation level versus strain in polycarbonate. The solid bold line shows the drive excitation level in mA (Y-axis) versus the strain level (X-axis). The harmonic ratio, if it existed over this strain interval would be plotted as well; as there were none observed, none are plotted. Note that the resonance curves show no peak bending, just as those for PVC.

Figure 3a. Elastic nonlinear behavior in a rock (3a) Acceleration versus frequency for nine excitation levels in Lavoux sandstone at ambient conditions. The large peak at 1234 Hz is artificially amplified to show the character of the linear behavior. (3b) Acceleration versus frequency for nine excitation levels in Fontainebleau sandstone at ambient conditions. The central portion of the figure shows the resonant peak bending for both upward (dashed lines) and downward (solid lines) frequency sweeps. The bottom and top plots show the corresponding time and frequency domain signals at low (but elastically nonlinear) drive level, and large drive level, respectively. The large peak at 1391 Hz is artificially amplified to show the character of the linear behavior.

Figure 4. Excitation level versus strain, and harmonic ratio versus strain in Lavoux limestone at 0.5% water saturation. The solid bold line shows the drive excitation level in mA (left-hand Y-axis) versus the strain level (X-axis). The harmonic ratio of each successive harmonic to the fundamental detected level is shown by the curved lines. The ratio values are shown on

the right-hand Y-axis, again versus strain. The ratios of the second U(f2), and third U(f3) harmonics relative the first harmonic U(f1) [the fundamental] are plotted. The curves associated with the harmonic data are second order polynomial fits shown to aid visualization of the data. In this case, only the second and third harmonics were measured although higher harmonics were present. Compare to Figure (2b) for polycarbonate where no harmonics were observed over this strain interval.

Figure 5. $|\Delta\omega/\omega_o|$ versus strain ε for (a) Meule sandstone, (b) Lavoux limestone, (c) St. Pantaleon limestone, (d) Fontainebleau sandstone, and (e) chalk at various saturation conditions in.

Figure 6. The cubic nonlinear parameter δ obtained from the third harmonic data for Berea sandstone.

Figure 7. Modulus calculated from time delay across the short direction of a sample of Fontainebleau sandstone during a typical sequence of resonance sweeps. Measurements were made near the bar center at near the bar end. The result shown was taken at the bar center; that at the bar end shows no change within our precision. Error bars are approximately two to three times the size of one dot.

Figure 8a. Resonant sweep data for both upward and downward sweep intervals for partially saturated chalk. Only a low drive and high drive level result are shown. The "linear" peak is not to scale, but has been expanded vertically. (8b) Excitation-strain-harmonic ratio data for dry chalk. (8c) $\Delta\omega/\omega_o$ versus strain versus harmonic ratio data for dry chalk (slightly different saturation than in figures (a) and (b). Both $\Delta\omega/\omega_o$ and the harmonic ratios have been normalized to their minimum values. Note the harmonic generation but minimal peak

bending. (8d) Comparative plot in using the same scale parameters for dry Lavoux. Note the peak bending and simultaneous harmonic generation.

Figure 9. Hypothetical stress-strain curve using calculated nonlinear coefficients from these experiments compared to those for "expected" values.

Tables

Material	Q	Length x Diameter (cm)	Slope of Frequency Shift Eq. (8)	Excitation-Strain Derivative	Harmonics Detected	Maximum Detected Strain
Sintered Aluminum	290	100. x 8.	UD[1]	linear	None	1.2×10^{-5}
Plexiglas	27	34. x 4.	UD	linear	2,3,4	4.4×10^{-6}
PVC a	59	120. x 8.	UD	linear	2,	3.0×10^{-6}
PVC b	59	61.2 x 10.5	UD	linear	2,4,3,6,5,7	5.3×10^{-6}
Aluminum	>50000	35. x 4.	UD	linear	2,3,4	2.2×10^{-5}
Pyrex Glass	2750	93.8 x 4.	UD	linear	2	2.2×10^{-5}
Polycarbonate	130	101.6 x 4.	UD	linear	2,3,4	1.1×10^{-4}

Table 1. Coefficients for elastically "linear" materials. Data shown, respectively, are inverse attenuation Q; sample length and diameters; the slope of the frequency shift from Eq. (8) which theoretically provides a measure of δ; the derivative of the excitation versus strain plot which is a measure of the modulus [It is only indicated whether or not the slope is linear (i.e., constant modulus and a linear equation of state)]; whether or not harmonics were detected in the time signal at resonance; and maximum detected strain levels. The numbers of the harmonics show which harmonics were detected and the relative dominance of observed harmonic amplitudes over the range of strain observation. For example, aluminum shows that the second, fourth and fifth harmonics were observed, and each successive harmonic amplitude over the range measured was relatively smaller in amplitude. On the other hand, PVCb shows that he fourth harmonic dominated over the third, etc. The PVC samples only differed in dimension.

[1]UD (UnDetectable) indicates that there was no detectable frequency shift using our apparatus.

Material	Q	S_w %	Length x Diameter (cm)	Slope of Frequency Shift Eq. (8)	|δ| (Harm-onic)	Excitation-Strain Derivative	Maximum Detected Strain
Estaillades Limestone	86	30	116.0x8.0	$-1.3x10^{10}$	$3.28x10^{10}$	NL	8.8x10-7
St. Pantaleon Limestone	140	42	115.0x8.0	$-3.4x10^{10}$		NL	1.1x10-6
St. Pantaleon Limestone	170	18	115.0x8.0	$-1.3x10^{10}$		NL	1.3x10-6
ASI Marble	360	~0	49.0x4.0	$-3.1x10^{9}$	$2.91x10^{9}$	NL	3.1x10-6
Chalk	225	~0	63.8x9.0	$-8.4x10^{10}$	$3.45x10^{14}$	NL	1.3x10-5
Meule	4.6	98	107.6x5.0	$-3.8x10^{9}$		Linear	1.7x10-5
Berea Sandstone	70	UK	30.1x5.0	$-4.1x10^{10}$		NL	1.4x10-6
Fontainebleau Sandstone	100	~0	39.0x4.0			NL	1.1x10-5

Table 2. Physical properties of various rocks, the shift of the slope ($|\Delta\omega/\omega_o|$ versus strain^2), the derivative of the excitation-strain curve (linear or NL nonlinear), and the maximum detected strain at the peak in resonance. S_w refers to saturation.

Material	Q	S_w %	slope frequency shift	$\|\delta\|$ (Harmonic)
Lavoux Limestone	1000	0.1	-7.36×10^{8}	-1.92×10^{9}
	820	0.5	-1.11×10^{9}	-3.59×10^{9}
	770	1.0	-1.26×10^{9}	-1.99×10^{9}
	700	1.5	-1.60×10^{9}	-9.10×10^{9}
	420	4.0	-1.11×10^{9}	-8.07×10^{9}
	440	5.0	-6.05×10^{9}	-1.72×10^{9}
	440	8.0	-4.62×10^{9}	-3.13×10^{9}
	330	20.0	-1.42×10^{10}	-1.45×10^{10}
	360	24.0	-9.15×10^{9}	-8.13×10^{9}
	350	31.0	-1.39×10^{10}	-1.21×10^{10}
	280	45.0	-1.13×10^{10}	-9.15×10^{9}
	300	50.0	-9.26×10^{9}	-1.32×10^{10}
	310	64.0	-2.04×10^{10}	-7.01×10^{9}
	150	73.0	-1.41×10^{10}	-6.24×10^{9}
	80	84.0	-1.31×10^{10}	-4.49×10^{10}
	45	98.0	-2.51×10^{11}	-9.56×10^{9}

Table 3. Physical properties as a function of saturation in Lavoux Limestone. Median value of δ shown from harmonic data.

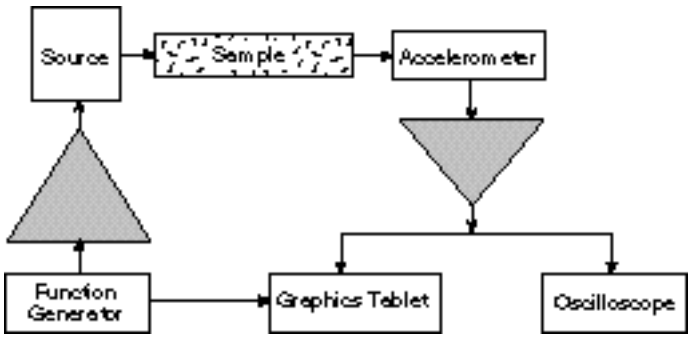
Source
Sample
Accelerometer
Function Generator
Graphics Tablet
Oscilloscope

Figure 1.

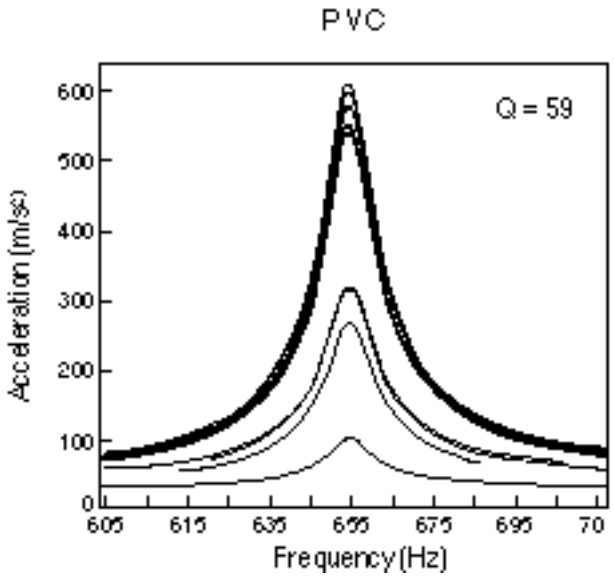
PVC
Q = 59
Acceleration (m/s²)
Frequency (Hz)
600
500
400
300
200
100
0
605
615
635
655
675
695
70

Figure 2a.

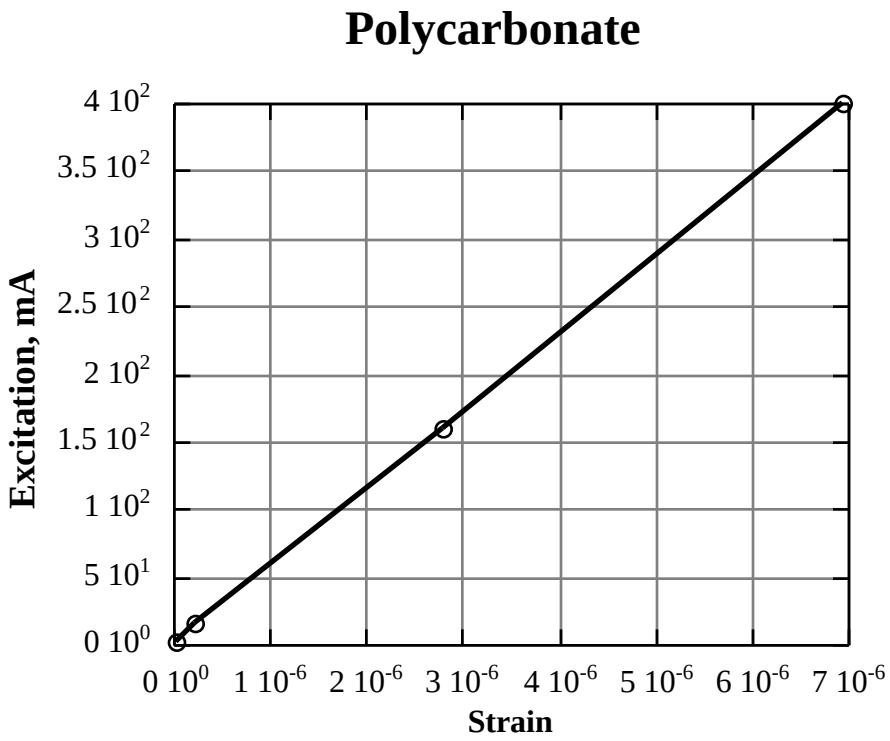
Polycarbonate
Excitation, mA
4 10^2
3.5 10^2
3 10^2
2.5 10^2
2 10^2
1.5 10^2
1 10^2
5 10^1
0 10^0
0 10^0
1 10^-6
2 10^-6
3 10^-6
4 10^-6
5 10^-6
6 10^-6
7 10^-6
Strain

Figure 2b.

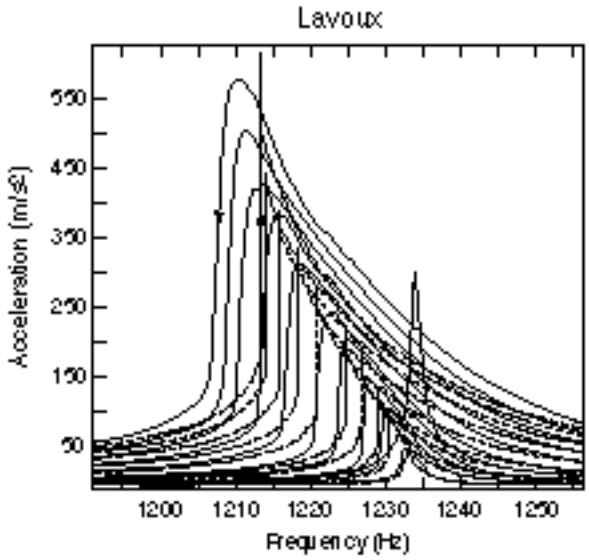
Lavoux
Acceleration (m/s²)
500
450
350
250
150
50
1200
1210
1220
1230
1240
1250
Frequency (Hz)

Figure 3a.

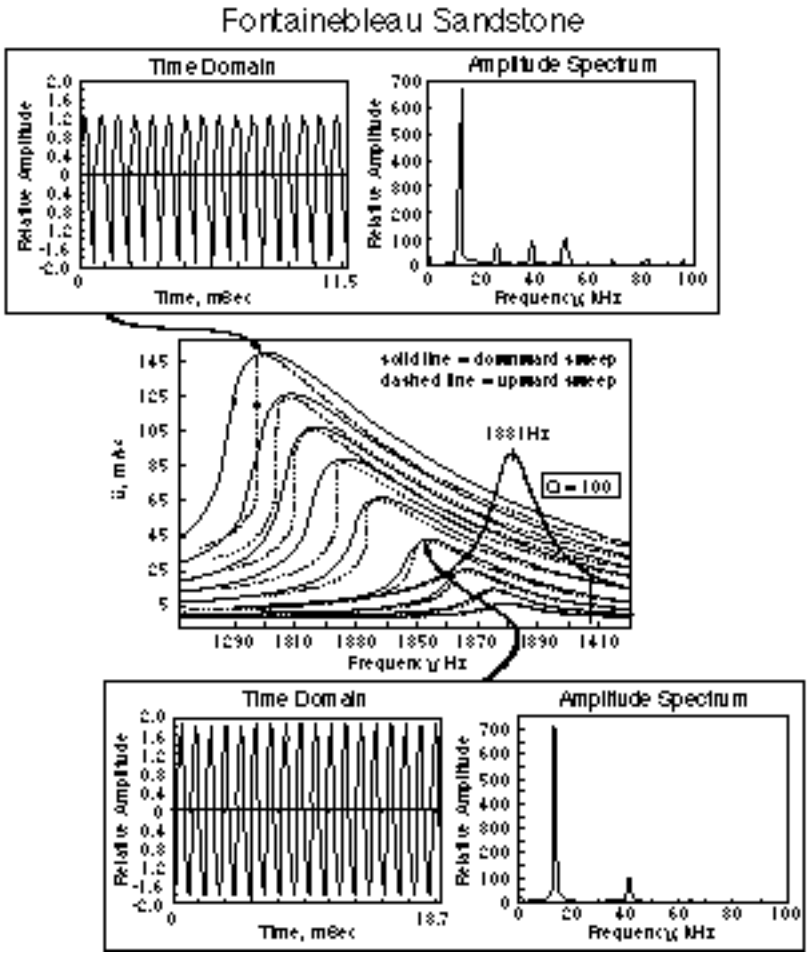
Fontainebleau Sandstone
Time Domain
Amplitude Spectrum
Relative Amplitude
Time, mSec
Frequency, kHz
solid line = downward sweep
dashed line = upward sweep
1881Hz
Q = 100
Frequency, Hz

Figure 3b.

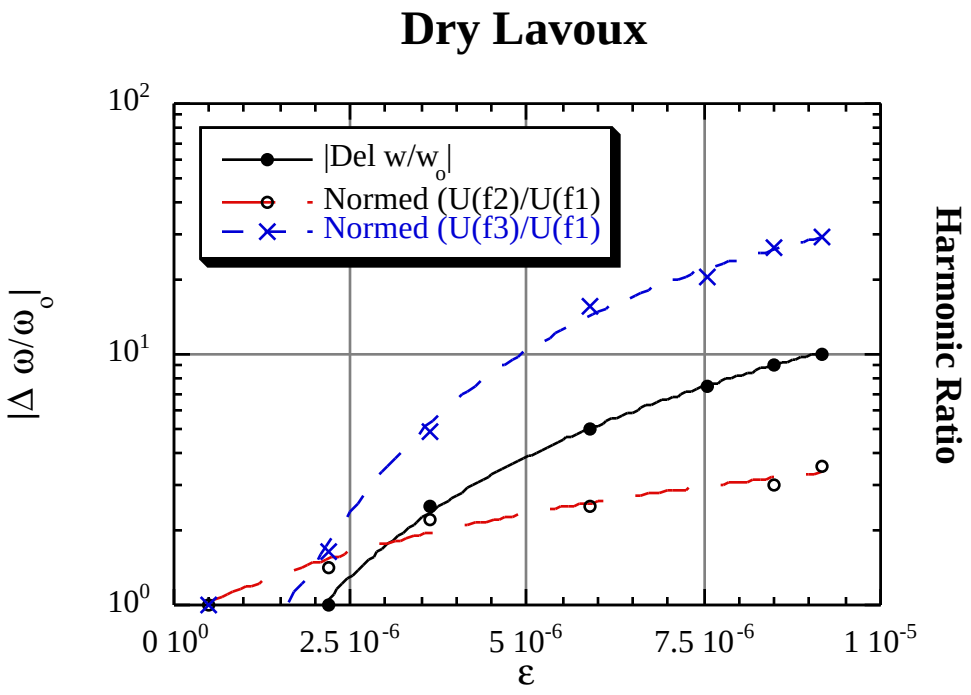
Dry Lavoux
|Del w/w_o|
Normed (U(f2)/U(f1)
Normed (U(f3)/U(f1)
|Δ ω/ω_o|
Harmonic Ratio
10^2
10^1
10^0
0 10^0
2.5 10^-6
5 10^-6
7.5 10^-6
1 10^-5
ε

Figure 4.

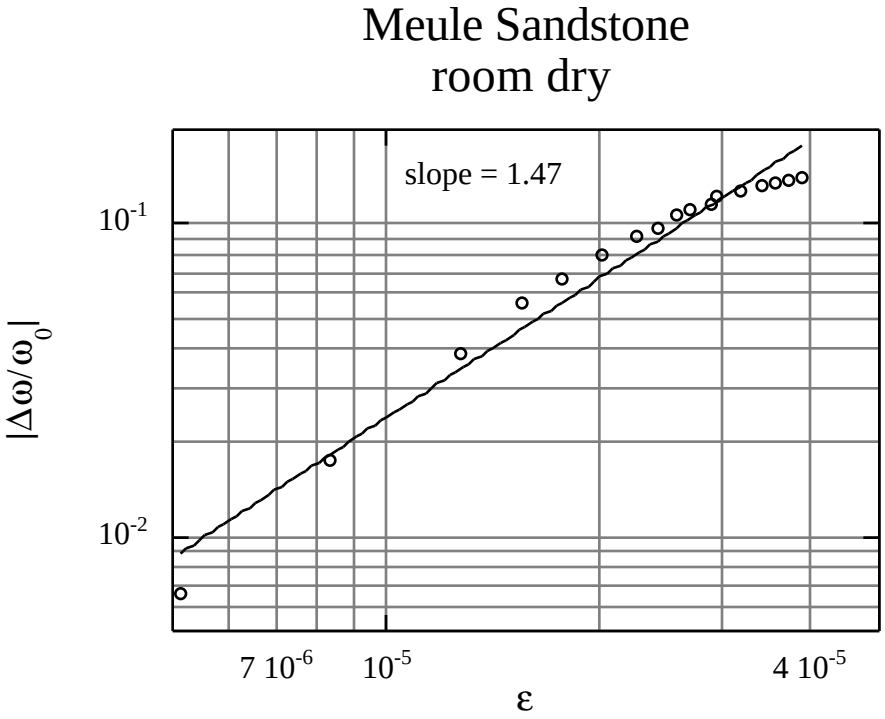

Figure 5a.

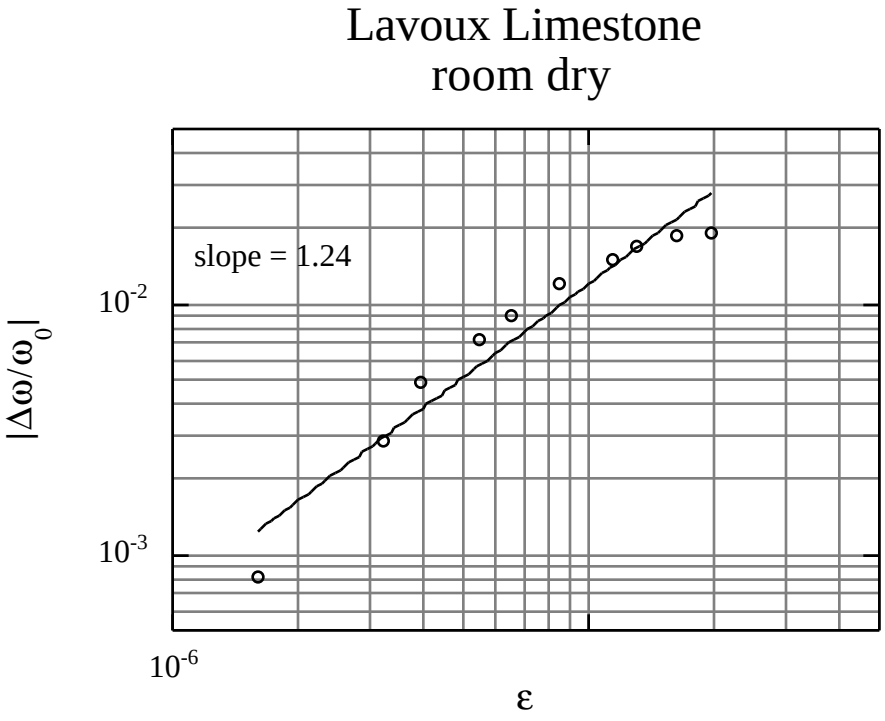

Figure 5b.

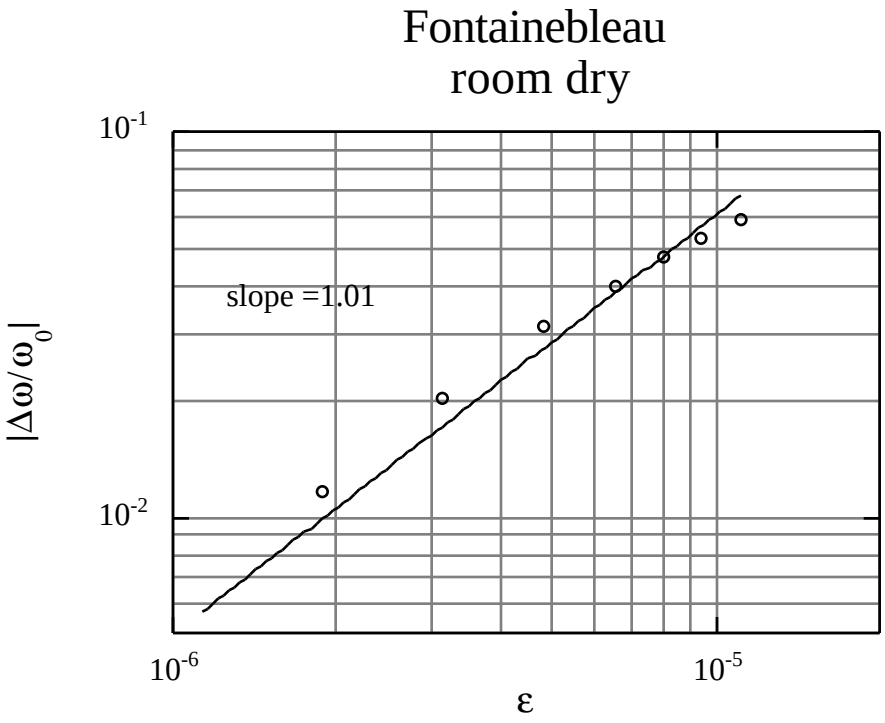

Figure 5c

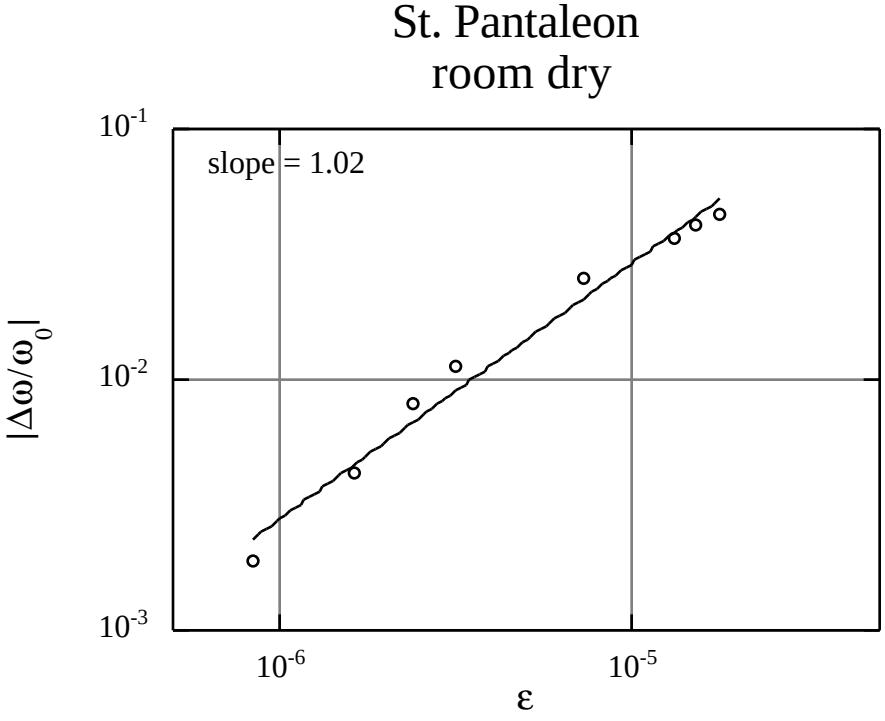

Figure 5d.

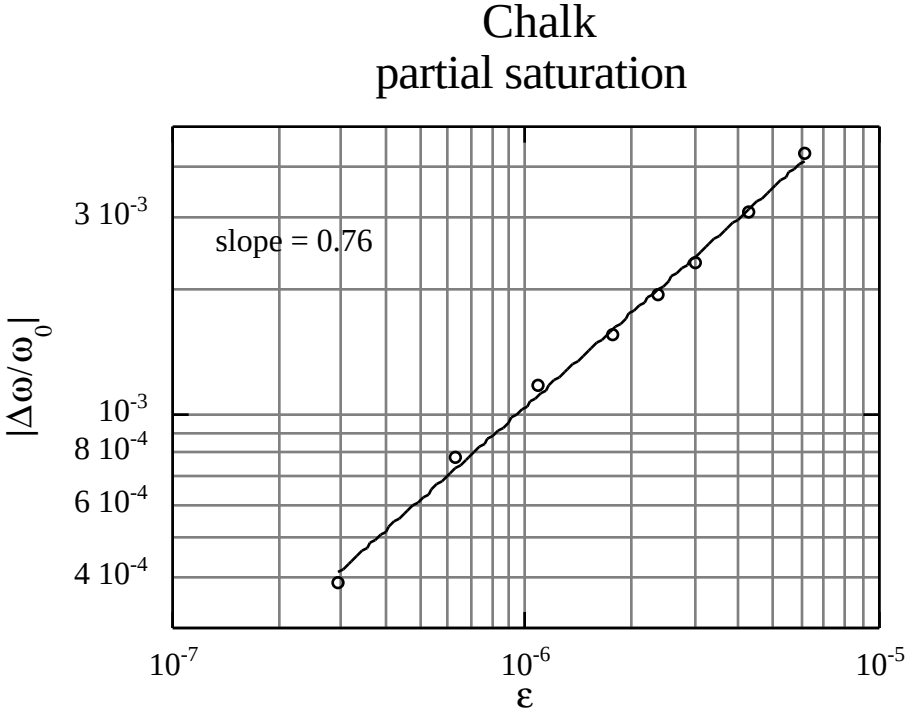
Chalk
partial saturation
slope = 0.76
3 10-3
10-3
8 10-4
6 10-4
4 10-4
|Δω/ω0|
10-7
10-6
10-5
ε

Figure 5e.

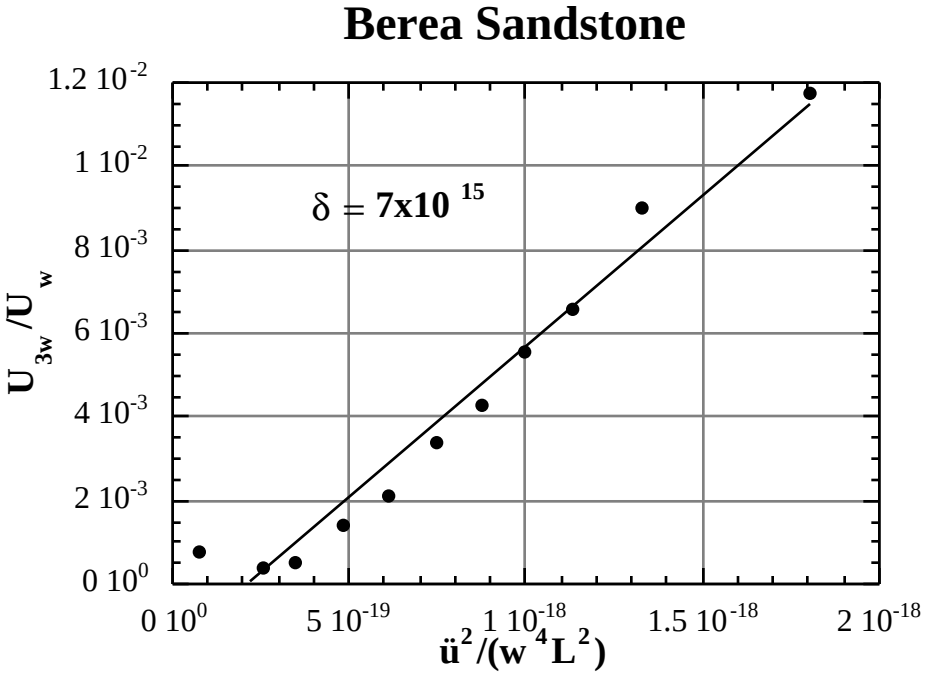
Berea Sandstone
δ = 7x10 15
U3w /Uw
ü2 /(w4L2)
1.2 10-2
1 10-2
8 10-3
6 10-3
4 10-3
2 10-3
0 100
0 100
5 10-19
1 10-18
1.5 10-18
2 10-18

Figure 6.

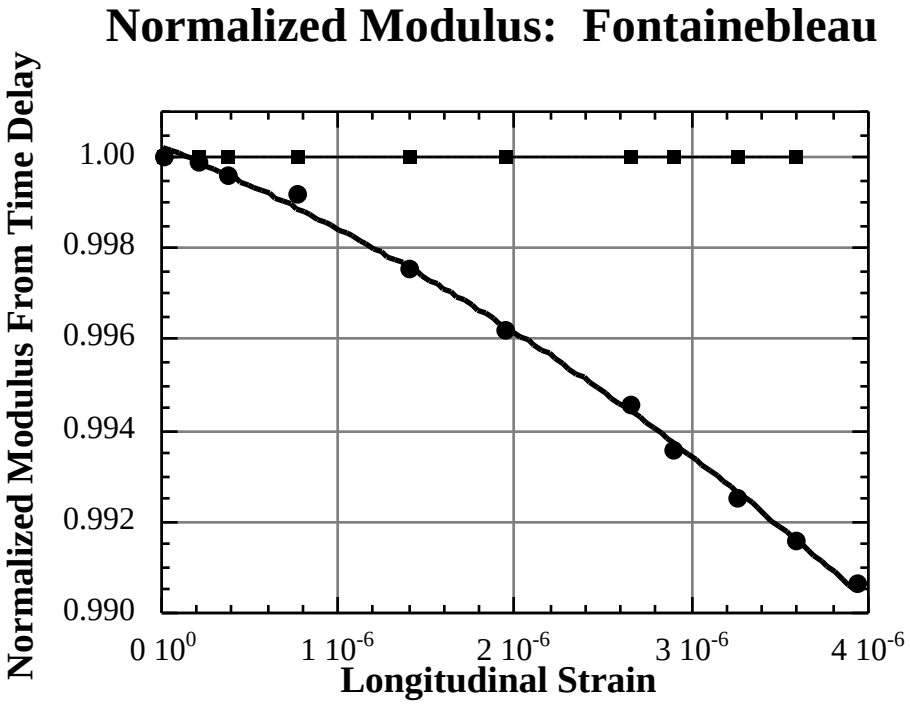
Normalized Modulus: Fontainebleau
Normalized Modulus From Time Delay
1.00
0.998
0.996
0.994
0.992
0.990
0 10^0
1 10^-6
2 10^-6
3 10^-6
4 10^-6
Longitudinal Strain

Figure 7.

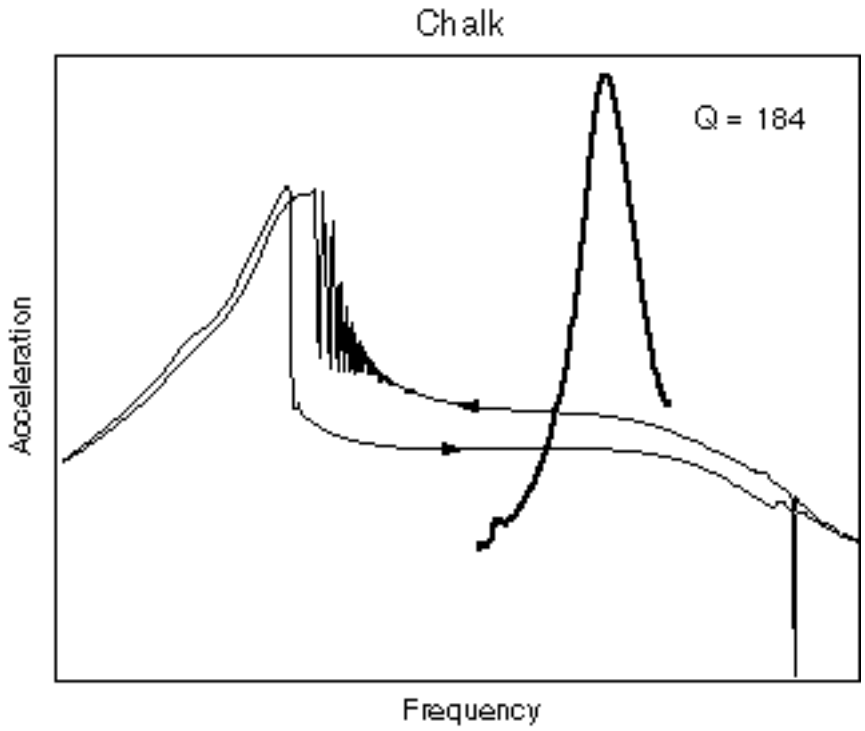

Figure 8a.

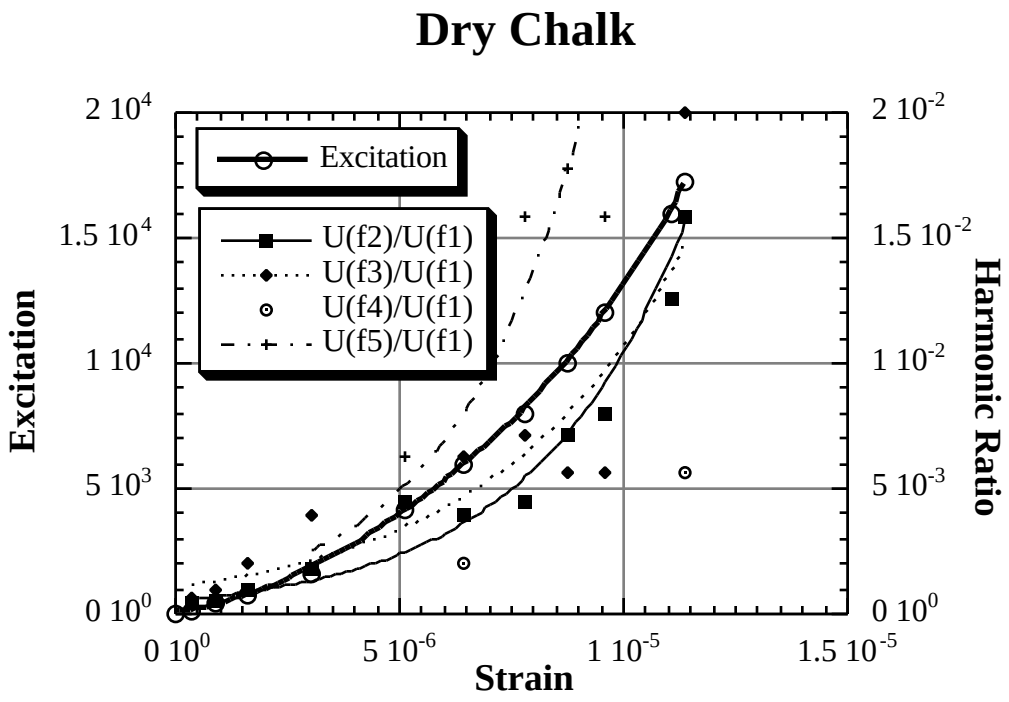
Dry Chalk
Excitation
U(f2)/U(f1)
U(f3)/U(f1)
U(f4)/U(f1)
U(f5)/U(f1)
Excitation
Harmonic Ratio
Strain
2 10^4
1.5 10^4
1 10^4
5 10^3
0 10^0
2 10^-2
1.5 10^-2
1 10^-2
5 10^-3
0 10^0
0 10^0
5 10^-6
1 10^-5
1.5 10^-5

Figure 8b.

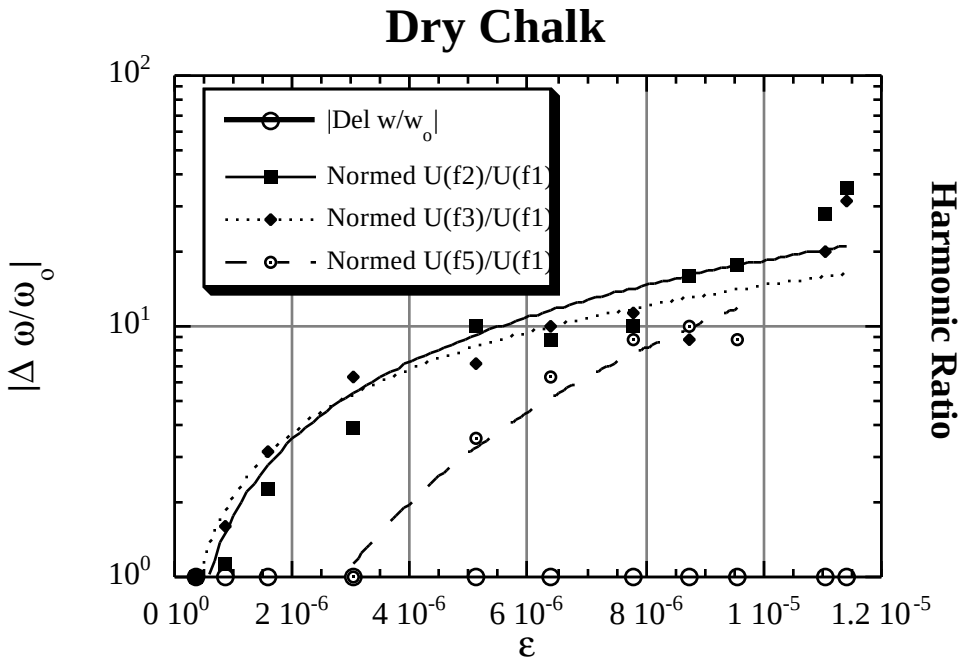
Dry Chalk
|Del w/w_o|
Normed U(f2)/U(f1)
Normed U(f3)/U(f1)
Normed U(f5)/U(f1)
|Δ ω/ω_o|
Harmonic Ratio
10^2
10^1
10^0
0 10^0
2 10^-6
4 10^-6
6 10^-6
8 10^-6
1 10^-5
1.2 10^-5
ε

Figure 8c.

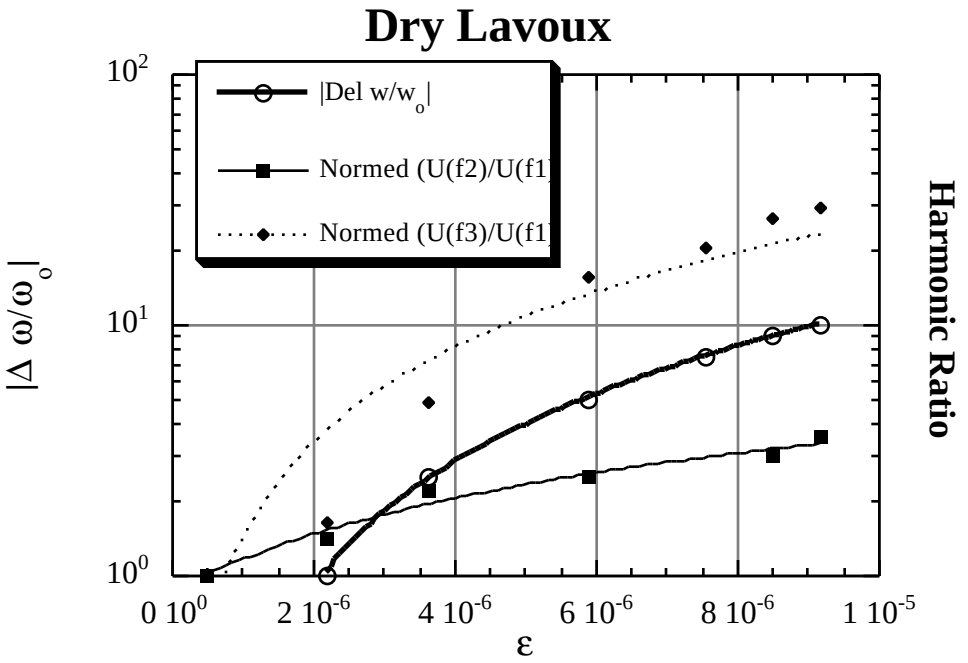
Dry Lavoux
|Del w/w_o|
Normed (U(f2)/U(f1)
Normed (U(f3)/U(f1)
|Δ ω/ω_o|
Harmonic Ratio
10^2
10^1
10^0
0 10^0
2 10^-6
4 10^-6
6 10^-6
8 10^-6
1 10^-5
ε

Figure 8d.

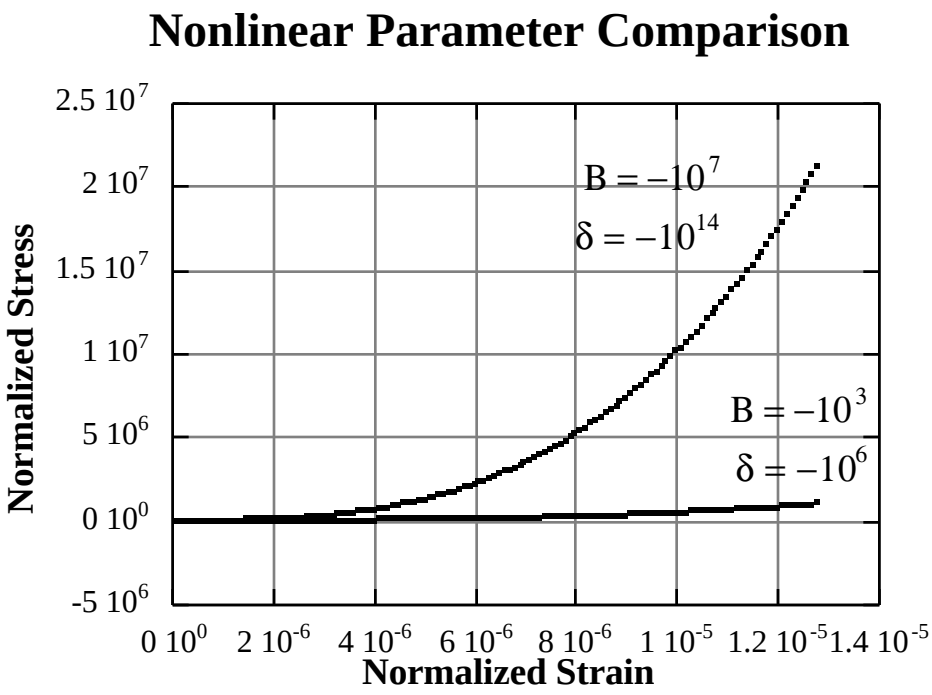
Nonlinear Parameter Comparison
Normalized Stress
2.5 10^7
2 10^7
1.5 10^7
1 10^7
5 10^6
0 10^0
-5 10^6
B = −10^7
δ = −10^14
B = −10^3
δ = −10^6
0 10^0
2 10^-6
4 10^-6
6 10^-6
8 10^-6
1 10^-5
1.2 10^-5
1.4 10^-5
Normalized Strain

Figure 9.